A STUDY OF LOCAL ATOMIC AND ELECTRONIC STRUCTURES OF AMORPHOUS ALLOYS BY MOSSBAUER SPECTROSCOPY

Supplement to Sci. Rep. RITU, A, June, 1978

A STUDY OF LOCAL ATOMIC AND ELECTRONIC STRUCTURES OF AMORPHOUS ALLOYS BY MÖSSBAUER SPECTROSCOPY

Hiromitsu Ino and Susumu Nanao

Institute of Industrial Science, University of Tokyo,

Roppongi, Minato-ku, Tokyo 106, Japan

ABSTRACT

Amorphous Pd-Si, La-Au and Fe base alloys were investigated by Mössbauer effect of ^{57}Fe and ^{197}Au nuclei, electrical resistivity and X-ray diffraction. It is concluded that the local atomic configurations of the amorphous alloys are close to those of the crystalline phases of the same composition. The electronic structures, the microscopic inhomogenities and the stabilities of the amorphous alloys were also studied.

INTRODUCTION

Atomic structures of various amorphous alloys have been investigated by many experimental techniques. X-ray and neutron diffraction studies determined the radial distribution functions and estimated the mean distances between component elements and the coordination numbers. Structural models based on dense random packing of hard spheres well explained the experimental results.

However, local atomic and electronic structures of the amorphous alloys are not yet clarified. Structural inhomogenities and stabilities of the alloys may be essentially related to them. It is, therefore, very important to get more knowledge on the physical quantities by Mössbauer effect, electrical resistivity and so on.

We studied following three groups of amorphous materials:
(1) Pd-Si alloys (Pd-Si-Fe, 12.5∿25at%Si, 0∿1at%Fe),
(2) Fe base alloys (Fe-P-C, Fe-P-B, Fe-Ni-B),
(3) La-Au alloys (La-Au-Fe, 18∿25at%Au, 0∿1at%Fe).

SAMPLE PREPARATION

Amorphous alloys were obtained by a two-piston type quenching apparatus. The specimens were levitation-melted by induction power and dropped between two pistons covered with mirror-polished silver plates. Thin foil

specimens, about 20 mm diameter and 30 ∿50 μm in thickness, were prepared. Chemical analysis of several specimens ensured that deviations of composition from nominal values were small.

X-RAY DIFFRACTION AND ELECTRICAL RESISTIVITY

X-ray diffraction measurements were made by a Rigaku roterflex diffractometar to detect the formation of amorphous and crystalline phases. Electrical resistivity measurements were carried out from 3 K to room temperature by a four terminal method. Superconducting transition behaviours and temperature coefficients of resistivity of La-Au alloys were examined.

MÖSSBAUER SPECTROSCOPY

The Mössbauer effect, *i*.e. the resonant absorption of recoilless γ-rays, is well suited to the study of local atomic and electronic structures in solids. Isomer shift (δ), the centre of gravity of the Mössbauer spectrum, is related to the electron density at the nucleus:

$$\delta = \text{const} \times (|\psi_A(0)|^2 - |\psi_S(0)|^2), \qquad (1)$$

where $\psi_A(0)$ and $\psi_S(0)$ are s-electron wave functions at the nucleus in absorber and in source, respectively.

Quadrupole splitting (ε) is the separation of a doublet in the spectrum caused by a coupling between nuclear quadrupole moment and crystalline electric field gradient (EFG) at the nucleus. EFG reflects the local asymmetry of the atomic configuration. Internal magnetic field, which is proportional to the unpaired s-electron density at the nucleus, gives us information on the magnetic surrounding around the probe atom and interactions with neighbouring atoms.

Mössbauer recoilless fraction, *i*.e. the probability of the resonant absorption of a γ-ray, is expressed by the equation, if we assume the Debye model,

$$f = \exp \left[- \frac{E_R}{k\theta_D} \left(\frac{3}{2} + \frac{\pi^2 T^2}{\theta_D^2} \right) \right], \text{ for } T \ll \theta_D, \qquad (2)$$

where E_R is the recoil energy of the free atom and θ_D is the Debye temperature.

Mössbauer effect measurements of ^{57}Fe were carried out at 77K and 300 K by a standard spectrometer. The 14.4 KeV γ-rays from ^{57}Co source were detected by a proportional counter. The line width of the spectrum for a thin iron absorber of 6 μm thickness was approximately 0.23 mm/s.

In Mössbauer effect measurements of ^{197}Au both ^{197}Pt source and absorber specimen were cooled to 18 K by a helium refrigerater. The ^{197}Pt sources were prepared by irradiating natural Pt metals in KUR reactor up to the dose of 1.5×10^{18} neutrons/cm^2. The 77.35 KeV γ-rays emitted from the excited state of ^{197}Au were counted by a Ge detecter with high energy resolution. The absolute value of recoilless fraction was precisely determined, since the disturbance due to X-rays from Pt and Au was sufficiently excluded.

PD-SI ALLOYS [1]

X-ray diffraction measurements of as-quenched specimens containing 15∿20at%Si exhibited only diffuse diffraction patterns corresponding to the single amorphous phase. While specimens with 12.5at%Si consisted of two phase mixture of amorphous phase and f.c.c. palladium solid solution, and those with 22.5 and 25at%Si were also mixture of the amorphous and Pd_3Si crystalline phases.

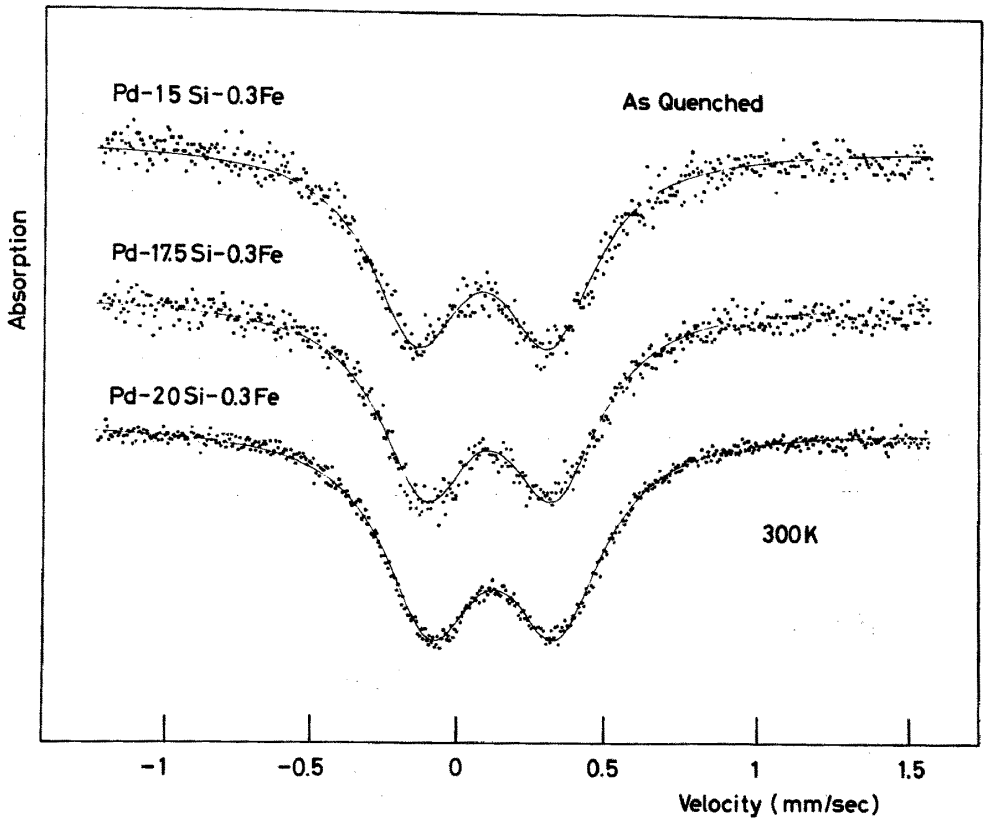

Fig.1 Mössbauer spectra for $Pd_{99.7-X}Si_XFe_{0.3}$ measured at 300K.

Fig.1 shows Mössbauer spectra at 300 K for $Pd_{99.7-X}Si_XFe_{0.3}$ with x = 15, 17.5 and 20. Each spectrum consists of two distinct sharp absorption peaks with nearly equal intensities. The peak separation becomes smaller and the centre of the spectrum shifts toward the positive velocity as the Si content increases. Solid curves in the figure are drawn by the least square fitting calculation assuming that the spectrum consists of two Lorentian curves with an equal intensity and half-width. The half-width of the peaks was approximately 0.38 mm/s, which is about 1.5 times of that for a standard thin absorber.

The same concentration dependences of quadrupole splitting and isomer shift were observed for the same specimens measured at 77 K. No magnetic hyperfine splittings were observed. The results of the Mössbauer effect measurements for the amorphous Pd-Si alloys are listed in Table 1, together with the data for the aged specimens.

Fig.2 illustrates the mean values of quadrupole splitting for the amorphous Pd-Si-Fe and crystalline $Pd_3Si(Fe)$. The quadrupole splitting in the amorphous alloys decreases linearly with the concentration of Si. The result shows that the atomic configuration around Fe atom, and also

Table 1

The values of isomer shift (δ) and quadrupole splitting (ε) for the quenched and aged Pd-Si-Fe alloys

specimen		δ (mm/s)		ε (mm/s)	
		at 77K	at 300K	at 77K	at 300K
$Pd_{84.7}Si_{15}Fe_{0.3}$	, as quenched	0.08_7	0.08_2	0.47_5	0.43_3
	, aged 120hr at 200°C	0.09_0	-	0.47	-
	, aged 500hr at 200°C	0.10_1	-	0.48	-
$Pd_{87.2}Si_{17.5}Fe_{0.3}$	, as quenched	0.11_6	0.10_7	0.45_3	0.41_4
	, aged 120hr at 200°C	0.11_8	0.11_1	0.45	0.42
$Pd_{79.7}Si_{20}Fe_{0.3}$	, as quenched	0.13_5	0.12_4	0.43_6	0.40_1
$Pd_{79}Si_{20}Fe_1$	, as quenched	0.14	0.13	0.43	0.40
	, aged 575hr at 200°C	0.13	0.13	0.43	0.40
	, aged 20hr at 250°C	0.14	-	0.41	-
	, aged 20hr at 275°C	0.14	-	0.41	-
	, aged 20hr at 300°C	0.14	-	0.43	-
$Pd_{74.7}Si_{25}Fe_{0.3}$ (crystalline Pd_3Si(Fe) phase)	, aged 20hr at 200°C	-0.10_4	-0.10_8	0.38	0.37
pure iron (reference)		0	0	0	0

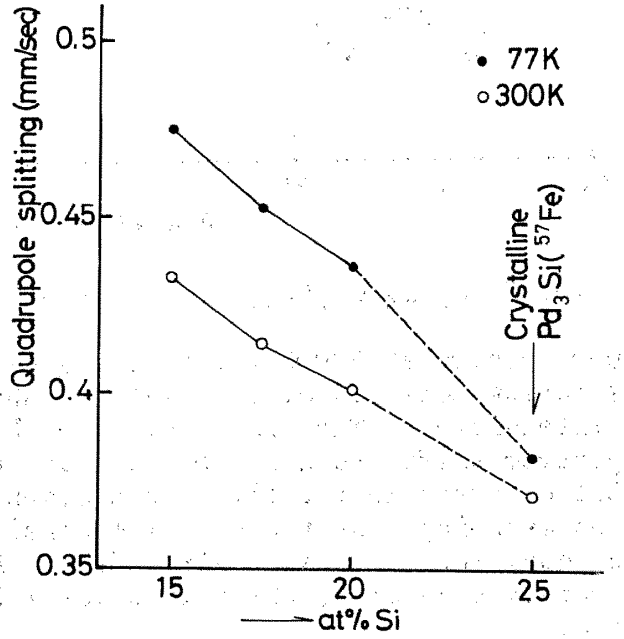

Fig.2 Quadrupole splitting of the amorphous $Pd_{99.7-X}Si_XFe_{0.3}$ and the crystalline Pd_3Si(Fe).

around Pd atom, changed with the Si content.

As shown in Fig.2, the values of quadrupole splitting for the crystalline Pd_3Si phase are nearly equal to those for the amorphous phase extrapolated to 25at%Si. Since quadrupole splitting is closely related to the atomic configuration of the nearest neighbouring atoms around the ^{57}Fe nucleus,

it is concluded that the average local atomic configuration of the amorphous Pd-Si phase are close to that of the crystalline Pd_3Si and that the difference in the configuration between the amorphous and crystalline phases is mainly caused by the difference in Si concentration of the materials. The conclusion that the short range order remains almost unchanged from the crystalline to the glassy states is also derived from a neutron diffraction experiment for $Pd_{80}Si_{20}$ [2] and a recent low temperature specific heat measurement for $Pd_{77.5}Si_{16.5}Cu_6$ [3].

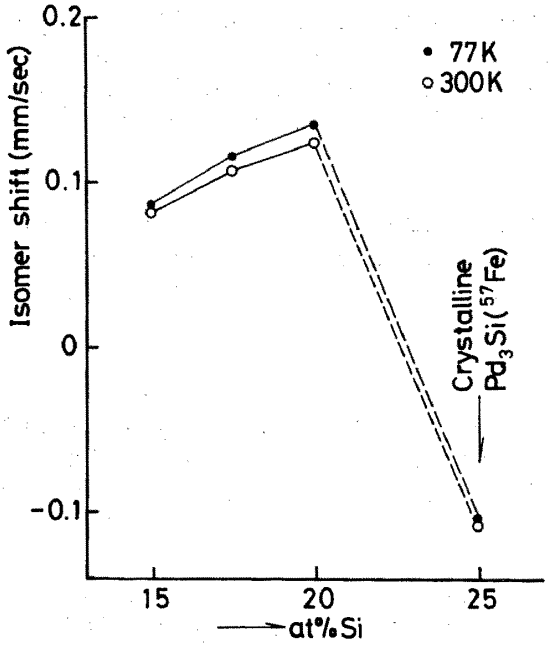

Fig.3 Isomer shift of the amorphous $Pd_{99.7-X}Si_X\ Fe_{0.3}$ and the crystalline Pd_3Si(Fe). The values of isomer shift is relative to α-iron measured at the same temperature.

Fig.3 shows the variation of isomer shift for the amorphous $Pd_{97.7-X}Si_XFe_{0.3}$ and crystalline Pd_3Si. The increase of isomer shift of the amorphous alloys with increasing Si content indicates that the S-electron density at the nucleus of iron atoms decreases with Si content. The result is consistent with the usual alloying effect of metalloid atoms and reasonably interpreted as follows. Metalloid Si atoms in the amorphous alloys offer their excess electrons to the d-band of the transition elements. Hence, the shielding effect against iron nuclei increases with increasing number of metalloid atoms, resulting in the decrease of S-electron density at the nuclei.

Isomer shift of ^{57}Fe in Pd_3Si (-0.1 mm/s) is significantly smaller than that of the amorphous phase. The bonding between Pd and Si atoms in Pd_3Si may have covalent-like nature and its valence band probably has a relatively narrow width. Therefore, the d-electron orbitals of foreign iron atoms will be unfavourable for bonding and can hardly accept the excess electrons of Si atoms. The shielding effect in Pd_3Si becomes weaker than in the amorphous state and then, the s-electron density at the nucleus increases.

The effect of iron addition on isomer shift and quadrupole splitting was very small in the dilute range of iron concentration (0.3∿1at%Fe) examined in our experiments (Table 1). On the other hand, remarkable

dependences of the Mössbauer parameters on the amount of iron addition have been observed by Sharon and Tsuei [4] in the range from 1 to 7at%Fe in $Pd_{80-Y}Si_{20}Fe_Y$, where the interaction between iron atoms plays important roles. The values of isomer shift and quadrupole splitting for their specimen containing lat%Fe agree well with ours. Hence, it is concluded that the interaction between iron atoms plays no significant roles in the dilute range and that the iron atoms have no direct contacts each other.

The ageing behaviours of the Pd-Si alloys were examined. After ageing 500 hr at 200°C, all X-ray diffraction profiles for the specimens containing 15∿20at%Si and 0∿1at%Fe were unchanged within experimental errors. The half-width value of the 1st diffuse peak remained approximately 5° for Cu K_α radiation during ageing, in contrast to the result by Masumoto and Maddin [5], where the half-width value decreases from 5° to about 1° before 100 hr ageing at 200°C.

The Mössbauer parameters were also unchanged by the same heat treatment as shown in Table 1. The difference in Si content and an addition of a small amount of Fe up to lat%Fe do not affect on the stability of the amorphous alloys at 200°C.

The specimens of the composition of $Pd_{79}Si_{20}Fe_1$ and $Pd_{80}Si_{20}$ were aged for 20 hr at 250°C, 275°C, 300°C and 350°C. Crystallization starts from the ageing at 250°C and almost finishes at 350°C. Lattice spacings of the specimen after ageing at 350°C coincide well with those of Pd_3Si and f.c.c. Pd phase, except for a few weak unknown peaks possibly due to surface oxides.

The ageing behaviours obtained in our experiments are consistent with the previous result by Duwez et al.[6], but quite different from that by Masumoto et al.[5,7]. It is suggested that the discrepancy arose from the difference in the microstructure of the examined amorphous materials prepared by different quenching techniques.

FE BASE ALLOYS [7]

Fig.4 shows Mössbauer spectra for the Fe-P-C system with different P and C concentrations. The Fe concentration in the three specimens remains nearly equal. The value of internal magnetic field increases with increasing C and decreasing P content. The obtained values of magnetic internal field and isomer shift at 77 K and 300 K for the Fe base amorphous alloys are listed in Table 2.

Yamauchi and Mizoguchi [8] proposed a model to explain the concentration dependence of the magnetic moment per 3d atom (Fe, Co) in amorphous metal-metalloid alloys. In the Y-M model, B, C and P are assumed to offer 1, 2 and 3 electrons per metalloid atom, respectively, to the d-holes of transition metals.

Alloy composition dependence of magnetic hyperfine field observed in our experiment is well explained in the Y-M model, although the quantitative agreement is insufficient. The values of isomer shift are, however, inconsistent with the electron-transfer model. The general relation between isomer shift of ^{57}Fe and 3d and 4s electron configuration was given by Walker et al.[9] (Fig.5). If the transfered electrons from metalloid atoms occupy the d-holes of an iron atom, isomer shift should be increased because of the shielding effect of the nucleus due to the increase of d-electrons.

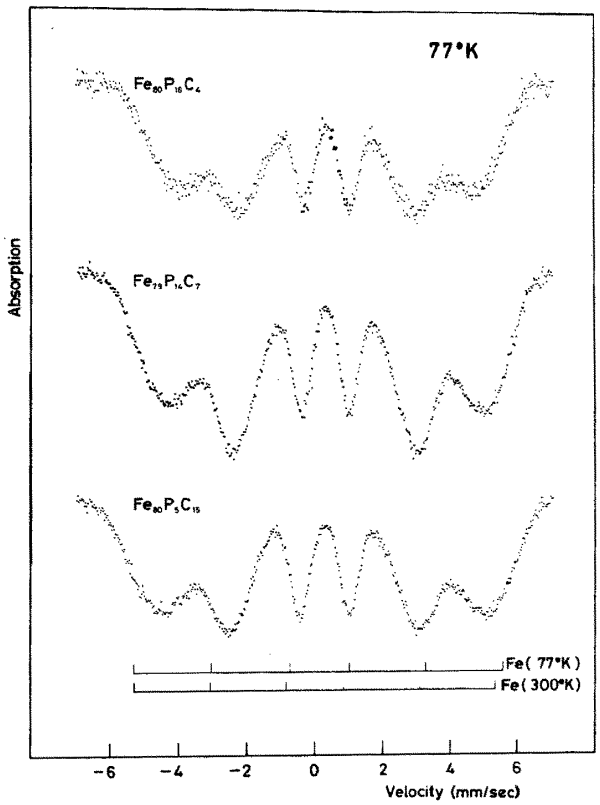

Fig.4 Mössbauer spectra for $Fe_{80}P_{16}C_7$, $Fe_{79}P_{14}C_7$ and $Fe_{80}P_5C_{15}$ measured at 77 K.

Table 2

The values of internal magnetic field (Hi) and isomer shift (δ) for Fe base amorphous alloys. The values of isomer shift is relative to α-iron measured at the same temperature.

Composition	Hi (KOe)		δ (mm/s)	
	at 300K	at 77K	at 300K	at 77K
$Fe_{80}P_{16}C_4$	238(0.72)	268(0.79)	0.19	0.25
$Fe_{79}P_{14}C_7$	253(0.77)	279(0.83)	0.185	0.23
$Fe_{80}P_5C_{15}$	268(0.81)	293(0.87)	0.13	0.19
$Fe_{78}P_{10}B_{12}$	277(0.84)	-	-	-
$Fe_{75}Ni_{11}B_{14}$	275(0.83)	-	-	-
$Fe_{65}Ni_{21}B_{14}$	269(0.82)	-	-	-
Fe	330(1.00)	337(1.00)	0	0

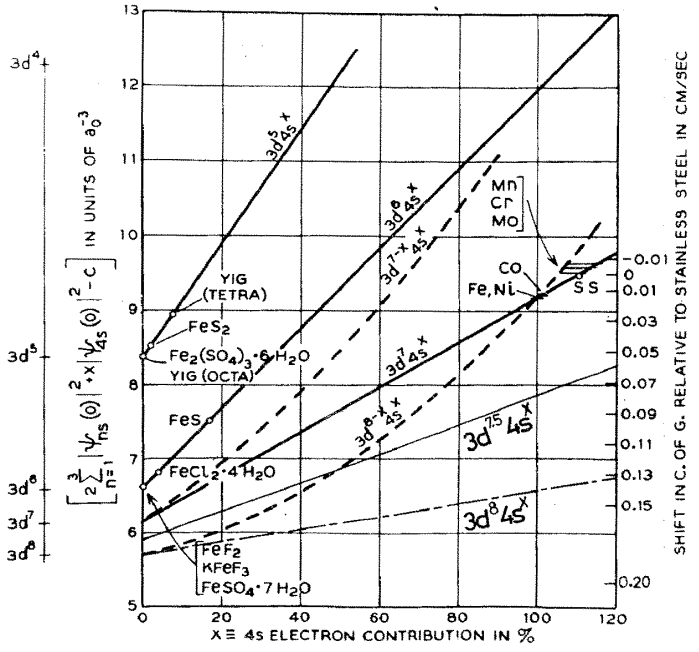

Fig.5 The relations between isomer shift and electron configuration of solids proposed by Walker et al.[9]. The lines of $3d^{7.5}4s^x$ and $3d^8 4s^x$ were added by the present authors.

For example, in the case of $Fe_{79}P_{14}C_7$, the number of transfered s-and p-electrons from P and C atoms is estimated by the Y-M model to be 0.7 per Fe atom. $3d^7 4s^1$, the electron configuration of pure iron, should be changed to $3d^{7.7}4s^{1.2}$. Then, the value of isomer shift is predicted to be 0.8 mm/s relative to pure iron according to the chart (Fig.6). However, the value experimentally observed is 0.20 mm/s.

The result means that the transfered electrons hardly contribute to the shielding of the iron nucleus despite of occupying the unpaired d-holes. It is suggested that most of the transfered electrons probably stay in the rooms between metal and metalloid atoms and make covalent-like bondings with sp-d mixture orbitals.

LA-AU ALLOYS [10]

The electrical resistivity was measured for the liquid-quenched $La_{82}Au_{18}$, $La_{80}Au_{20}$ and $La_{78}Au_{22}$ alloys, in which ^{57}Fe-enriched iron was doped about 0.5 at%. The results in low temperature region are shown in Fig.6. The X-ray diffraction profiles are also shown in Fig.7.

The $La_{82}Au_{18}$ specimen, which is identified to be the mixture of the crystalline and the amorphous phases, presents a sharp ($\sim$0.1 K) superconducting transition. The crystalline phase, which has higher superconducting transition temperature than the amorphous phase, probably forms short-passes in the specimen. The $La_{78}Au_{22}$ specimen also presents a sharp transition at a lower temperature. We can indentify this specimen to be a homogeneous amorphous alloy.

On the other hand, the $La_{80}Au_{20}$ specimen, which is identified to be a homogeneous amorphous phase only from the X-ray profile in Fig.7, has multi-stages in the superconducting transition as shown in Fig.6. The

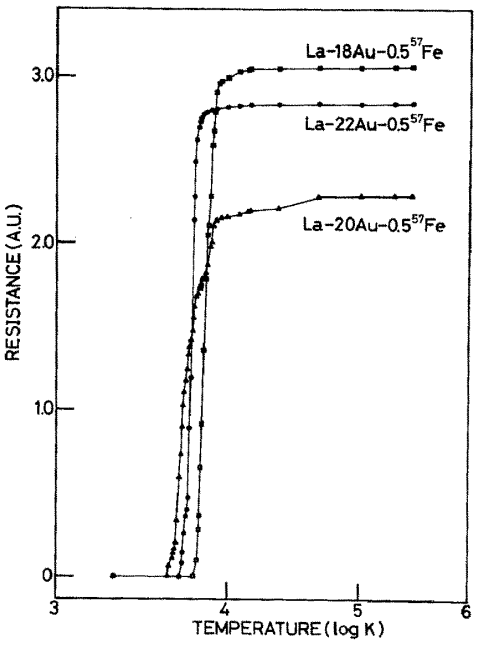

Fig.6 Electrical resistivity at superconducting transition of liquid quenched La-Au alloys.

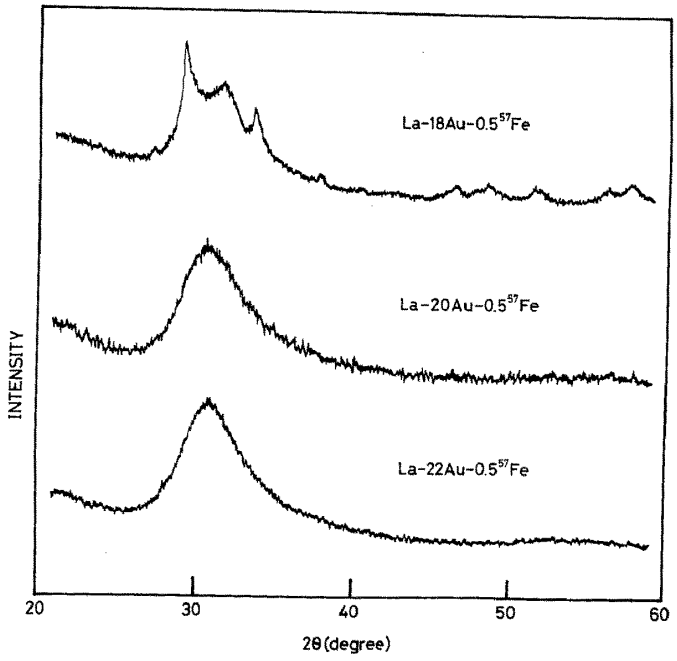

Fig.7 X-ray diffraction profiles of liquid quenched La-Au alloys.

stages are probably attributed to the inhomogeneity of the specimen such as the spatial fluctuation of concentration and the micro-crystalline phase dispersed finely in the matrix of the amorphous phase.

The transition temperatures for the crystalline and amorphous phases in the figure were affected by a small addition of magnetic (iron) impurities. The systematic change in the transition temperature with Au composition was obtained for the liquid-quenched binary La-Au alloys in the wide range of Au concentration (2 ∿ 25at%Au).

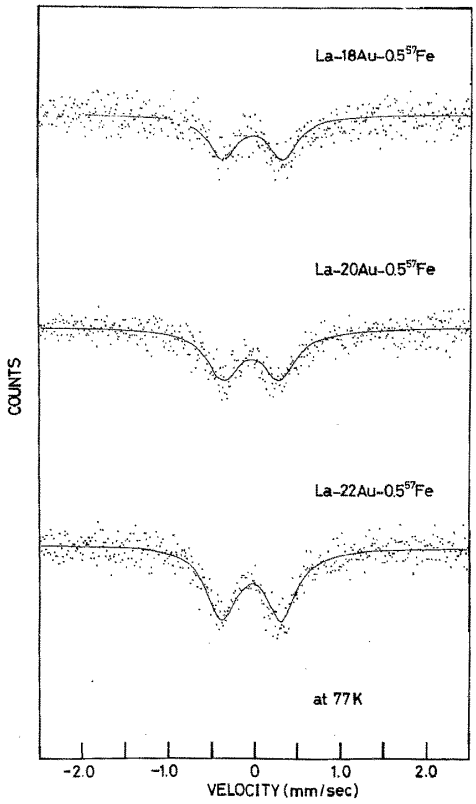

Fig.8 Mössbauer spectra of ^{57}Fe nuclei for liquid quenched La-Au alloy measured at 77 K.

The Mössbauer spectra of ^{57}Fe nuclei for the same specimens as in Fig.6 and 7 are shown in Fig.8. The peak width, isomer shift and quadrupole splitting were not changed appreciably with the difference in microstructure and Au concentration. The inhomogeneity was not detected by Mössbauer spectroscopy.

Fig.9 shows the Mössbauer spectra of ^{197}Au for the amorphous and crystallized (annealed 3hr at 350°C) $La_{78}Au_{21.5}Fe_{0.5}$ specimen measured at 18 K. The peak width and the quadrupole splitting are larger in the amorphous phase than in the crystallized one. The values of the isomer shift are nearly the same (7.7 mm/s and 7.8 mm/s). These two values are also close to that of dilute Au in La (8.1 mm/s) [11].

The above mentioned results of ^{57}Fe and ^{197}Au Mössbauer spectroscopy suggest that the atomic configurations around Au atoms are very similar between the amorphous and crystalline phases, although slightly different atomic configurations exist in the former phase causing the broadening of the Mössbauer peaks. The fact that the values of the isomer shift of ^{197}Au in the amorphous alloy and the dilute La-Au alloy are close together also suggests that Au atoms in the amorphous phase have no direct contacts as in the dilute alloy. The same conclusion has been derived from the radial distribution function estimated from X-ray diffraction measurements [12].

The recoilless fraction of ^{197}Au in the amorphous phase is smaller about 14% than that in the crystallized phase, reflecting the difference in the phonon spectrum. The Debye temperatures for the amorphous and crystallized specimens were estimated to be 110 K and 116 K, respectively, by a preliminary calculation.

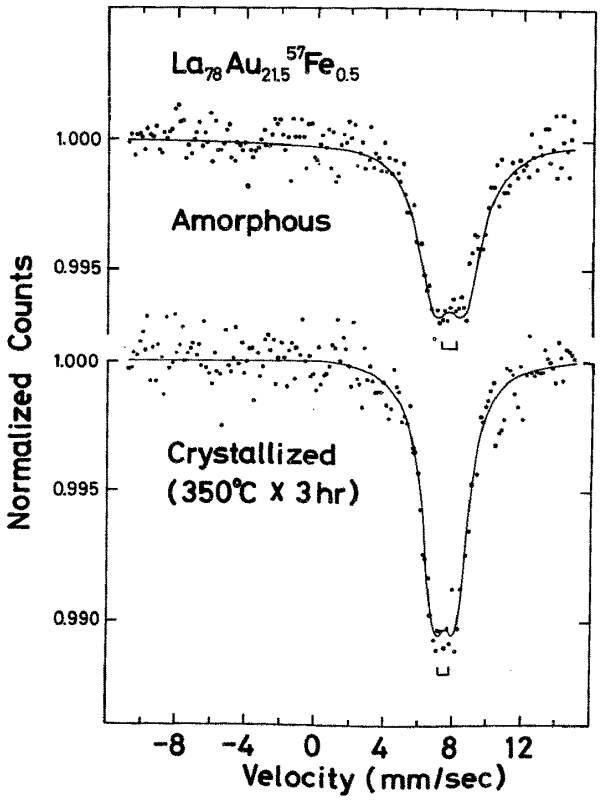

Fig.9 Mössbauer spectra of ^{197}Au nuclei for amorphous and crystallized $La_{78}Au_{21.5}Fe_{0.5}$.

ACKNOWLEDGEMENT

The authors express their thanks to Mr. Muto, Mr. Ohji and Mr. Sugiura for cooperation in the experiments.

REFERENCES

[1] H. Ino, S. Nanao and T. Muto : Submitted to Acta Met. in a full paper form.

[2] K. Suzuki, T.Fukunaka, M. Misawa and T. Masumoto : Mat. Sci. Eng. 23, 215(1976).

[3] J. C. Lasjaunias, A. Ravex and D. Thoulouze : To be published (private communication).

[4] T. E. Sharon and C. C. Tsuei : Solid State Comm. 9, 1923(1971).

[5] T. Masumoto and R. Maddin : Mat. Sci. Eng. 19, 1(1975).

[6] P. Duwez, R. H. Willens and R. C. Crewdson : J. Appl. Phys. 36, 2267 (1965).

[7] S. Nanao, K. Muto, T. Namiki and H. Ino : Annual Meeting of Japan Inst. Metals, Symposium, Oct. 1976, Preprint p67.

[8] K. Yamauchi and Mizoguchi : J. Phys. Soc. Japan 39, 541(1975).

[9] L. R. Walker, G. K. Wertheim and V. Jaccarino : Phys. Rev. Letters 6, 98(1961).

[10] S. Nanao, J. Sugiura, Y. Ohji and H. Ino : Submitted to 3rd Int. Conf.

on Rapidly Quenched Metals held at Succex (1978).

[11] F. E. Wagner, G. Wortmann and G. M. Kalvius : Phys. Letters 42A, 483 (1973).

[12] J. Logan : Scripta Met. 9, 379(1975).